Chemical Engineering Journal 95 (2003) 241–249

Chemical Engineering Journal

www.elsevier.com/locate/cej

Adsorption of carminic acid, a dye onto glass powder

G. Atun*, G. Hisarli

Department of Chemistry, Faculty of Engineering, Istanbul University, Avcilar 34 850, Istanbul, Turkey

Abstract

The adsorption of carminic acid (CA) on glass powder (GP) has been studied polarographically. The adsorption is a two-stage process comprising a fast initial phase and a slower second phase. The rate constant for the first phase increased slightly with increasing dye concentration while the rate constant for the second phase remained almost constant. This indicated the presence of two diffusional processes. In the first phase, CA molecules are adsorbed at the outer sites of the glass particles in a fast process that dominates the initial kinetics of adsorption. In the second phase, dye molecules slowly diffuse inward and adsorb to the inner sites of the glass particles. The rate of adsorption increases with increasing temperature. The thermodynamic parameters for activated state have been evaluated using the Arrhenius and Eyring equations. The equilibrium isotherms have been analyzed using the Freundlich and Langmuir equations. The parameters of the isotherms show that the adsorption process is favorable.

Keywords: Carminic acid; Glass powder; Adsorption kinetics; Freundlich isotherm; Langmuir isotherm

1. Introduction

The adsorption of several anionic dyes such as D&C Red #6, Naphtol Yellow S (Acid Yellow #1), Acid Blue #25 and Guinea Green B onto alumina-modified silica particles has been studied in order to prepare nanosize pigments for special applications such as ink-jets and color filters for flat panel displays [1]. Reactive dyes have also been grafted to derivatized silica surfaces to produce water dispersible pigments for ink-jet applications [2].

Carminic acid is an anionic, anthraquinone-based food coloring dye. Since CA is relatively water soluble and nontoxic, it forms a model compound for investigation the recovery of organic chemicals utilizing adsorption techniques [3]. Sahm et al. underlined the usefulness of direct current (dc) polarography for the determination of anthraquinone-based dyes [4]. For these dyes, reversible reduction waves are observed for the two-electron reduction of the anthraquinone moiety in acidic medium [5–8]. The diffusion current of the reduction wave linearly increases with increasing dye concentration. The dye content of the dispersion can, therefore, be determined in without any separation procedures such as centrifugation or filtration.

The rate of adsorption of an adsorbate onto porous adsorbents depends on three essential steps: (i) external film diffusion across the boundary layer, (ii) adsorption at a surface site and (iii) internal mass transfer within the particle-based pore diffusion or solid surface diffusion mechanism [9–12]. One or more of these processes may be involved in the rate-determining step. Many kinetic models have been developed for predicting the performance of adsorption systems [12–16].

The zeta potential measurements have been applied to the study of the adsorption of cationic and anionic organic species onto glass. When a cationic species is adsorbed onto glass, the zeta potential is reversed from the negative value intrinsic to the glass surface to a positive value. Adsorption of an anionic species, however, increases the negative zeta potentials [17]. In a previous study, it was shown that a modified glass surface exhibits high adsorption capacity for safranin O, a cationic (basic) dye [18]. One of the current research focuses, however, is the removal of acid dyes from colored effluents using a variety of adsorbents. This focus is due to the fact that these dyes are commonly found in aqueous effluent arising from the printing plants of textile industries [19–24]. Fine particles of glass can be well dispersed in aqueous solution, and the chemical structure of glass (which contains both SiO_2 and Al_2O_3) suggest that GP will demonstrate high adsorption affinity for acid dyes. In this study, we have used CA as a model molecule for acid dyes in oder to study adsorption onto glass powder.

* Corresponding author. Tel.: +90-212-4212543; fax: +90-212-5911997.
E-mail address: gultena@istanbul.edu.tr (G. Atun).

1385-8947/$ – see front matter
doi:10.1016/S1385-8947(03)00110-4

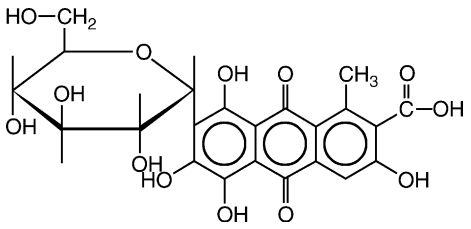

Fig. 1. Molecular structure of CA.

2. Experimental materials and methods

2.1. Adsorbate specifications

Carminic acid (Fig. 1) is an acid anthraquinone dye (7-C-α-glucopyranosyl-3,5,6,8-tetrahydroxy-1-methyl-2-anthraquinone carboxylic acid, C.I. 75470, Natural Red 4). It was purchased from Sigma (90% pure) and used as received.

2.2. Adsorbent specifications

The glass sample employed as adsorbent has the following chemical composition by weight: SiO_2, 72.5%; Al_2O_3, 1.2%; Fe_2O_3, 0.37%; TiO_2, 0.173%; CaO, 7.82%; MgO, 3.96%; Na_2O, 13.64%; and K_2O, 0.26%.

We have determined the pH_{pzc} for GP to be 3.97 by a potentiometric titration method at 298 K. A GP suspension of 1 g l^{-1} in 25 cm^3 electrolyte medium of 0.1 M NaCl and 0.1 M HCl was prepared. After equilibration for 24 h, the suspension was back-titrated with carbonate-free 1 M NaOH using a Metrohm E 485 titrator. The pH measurements were carried out with a Jenway pH meter equipped with a combined glass electrode. The acidic supernatant was utilized as the system blank and titrated with hydroxide in a manner identical to that of the sample suspension. Surface charge density (σ) on hydrous oxides is defined by the net uptake of protons, i.e. $\sigma = F(\Gamma_{H^+} - \Gamma_{OH^-})$, where Γ_{H^+} and Γ_{OH^-} are the moles of H^+ and OH^- ions adsorbed per unit surface area, and F is the Faraday constant. The value of pH_{pzc} was determined from the σ–pH curve to be the pH at zero net adsorption of protons and hydroxide ions, i.e. $\Gamma_{H^+} - \Gamma_{OH^-} = 0$.

2.2.1. Pore-size distribution

Data obtained from nitrogen desorption isotherms by employing a Quantachrome Autosorb Automated Gas Sorption System were used to calculate the BET surface area, pore area and pore-size distribution of the GP. Pore-size distribution was calculated using Autosorb for Windows version 1.19 and is shown in Fig. 2. GP contains mainly mesopores with a pore-size range of 16–37 Å. The mesopore area and BET surface area of the GP are determined to be 2.28 and 2.37 $m^2\,g^{-1}$, respectively.

2.3. Adsorption experiments

A 25 cm^3 aliqout of acetic acid–sodium acetate buffer at pH 4 was placed in the water-jacketed polarographic cell, and the solution was purged with nitrogen for 15 min. The

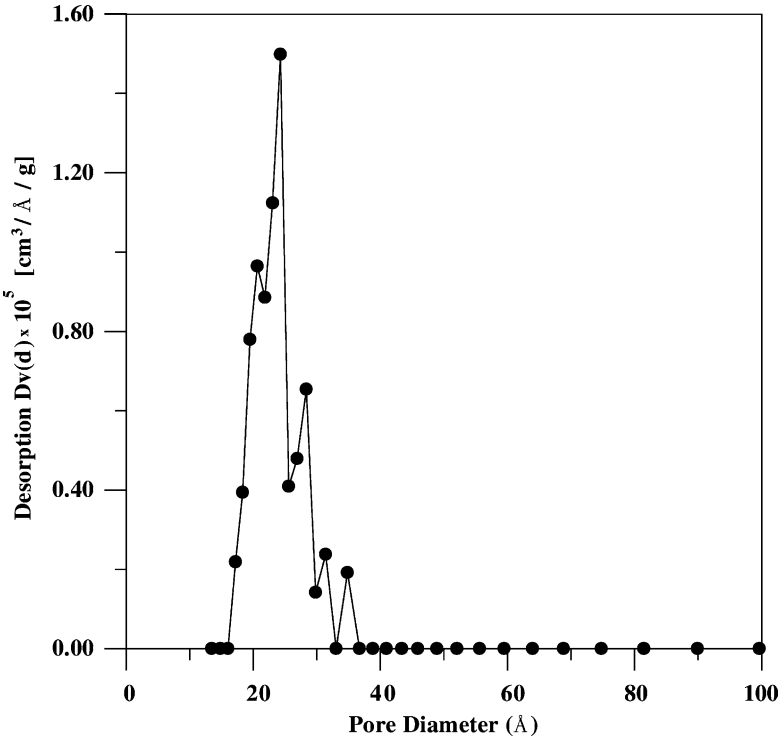

Fig. 2. Pore size distribution for the GP.

mercury drop time was adjusted to 2.7 s per drop. Solutions were prepared by adding sufficient CA into buffer solution to obtain initial concentrations in the range of 1×10^{-4} to 1×10^{-3} M, and polarographic curves were recorded using a Radiometer Copenhagen PO-4 polarograph. Next, 0.25 g of adsorbent was added into the solution, and polarograms were taken at various time intervals. The particle size of adsorbent was maintained at 40–125 μm. The solutions were stirred by nitrogen gas bubbling during the adsorption experiments. A well-developed, reproducible cathodic wave was observed which corresponded to a reversible, two-electron reduction process ($E_{1/2} = -0.55$ V).

The fraction of dye removal from solution was determined from the limiting current of this wave using the relation:

$$F = \frac{i_i - i_t}{i_i} \quad (1)$$

where i_i and i_t are the limiting currents of the cathodic wave of the CA solution initially and at time t, respectively.

The amount of adsorbed dye (in mol g^{-1}) was calculated using the following relationship:

$$Q = C_i F \frac{V}{m} \quad (2)$$

where C_i is the initial concentration of the dye solution (in mol dm^{-3}) and V/m the ratio of the solution volume to the mass of the adsorbent (in dm^3 g^{-1}).

Equilibrium isotherms were derived from data obtained at 293 K with a fixed V/m ratio (0.1 dm^3 g^{-1}) and at the different initial CA concentrations mentioned above.

3. Results and discussion

3.1. Adsorption kinetics

The effect of contact time on the amount of dye adsorbed is presented in Fig. 3 for various initial concentrations of CA. The adsorbed fraction was found to decrease while the total amount of adsorbed dye increased with increasing initial concentrations of CA. Similar results for the extent of removal of dyes from solution have been reported in the literature [25]. This behavior is attributed to the fact that there are reductions in immediate solute adsorption due to the lack of enough available open sites to adsorb high initial concentrations of dye.

Initially, the amount of CA adsorbed onto the glass surface increases rapidly, but then the process slows down. The adsorption kinetics of CA onto GP have been studied by applying the following kinetic approximations proposed by H. McKay [9] and Boyd et al. [10]:

The rate constants of the adsorption reactions can be calculated using the McKay equation:

$$\ln(1 - F) = -kt \quad (3)$$

The values obtained for $\ln(1 - F)$ as a function of time t, are plotted in Fig. 4. In order to analyze the curve, the final linear portion is extrapolated back to $t = 0$. Upon subtraction of the extrapolated line from the original curve, another straight line is obtained which represents the initial reaction. The overall adsorption is seen to consist of a fast initial process followed by a slower process that completes the adsorption. The rate constant of the initial fast reaction (k_1) is calculated from the slope of the first straight line (see the inset in Fig. 4). The existence of two straight lines indicates two processes. A faster process corresponding to the residual curve, and a slower one corresponding to the later linear portion of the McKay plot, contribute to the overall rate of adsorption. As can be seen from Fig. 4, the rate constant of the slower reaction (k_2) is determined from the slope of the second linear portion.

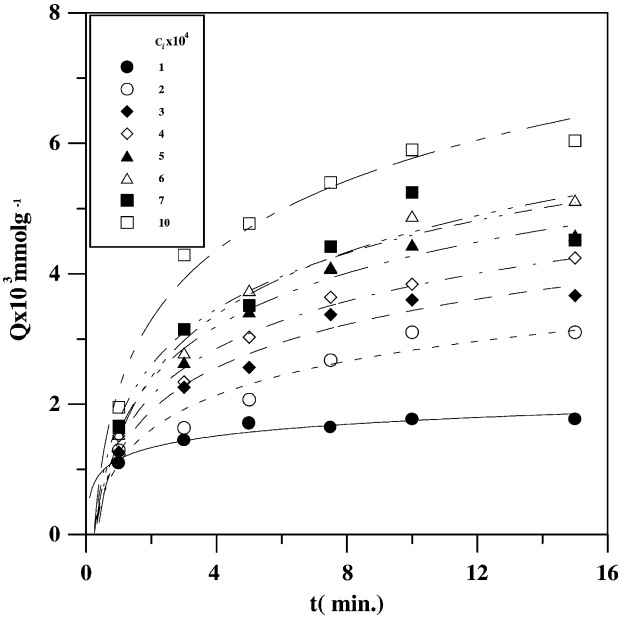

Fig. 3. Effect of contact time on CA adsorbed at various initial concentrations in the range of 1×10^{-4} to 1×10^{-3} M at 293 K.

The effect of initial dye concentration on the rate of adsorption by GP is shown in Fig. 5. It is evident from Fig. 5 that the rate constants of the initial fast reaction increase linearly with concentration and that the reaction is controlled by film diffusion. The values of k_2 are approximately 1000 times smaller than k_1 values and are not concentration dependent ($k_{2(\text{mean})} = 5.06 \pm 0.75 \times 10^{-5}$ s^{-1}). Since particle diffusion is characterized by an adsorption rate that is independent of solute concentration, the obtained k_2 values are evidence of a particle diffusion mechanism in the second step of the adsorption [10,11].

Assuming that all particles were uniform spheres of radius r, the expression developed by Boyd et al. for the particle diffusion controlled kinetics correlates the fractional attainment F', at time t with the radius, r, of the adsorbent particles of the ingoing ions as

$$F' = \frac{Q_t}{Q_\infty} = 1 - \frac{6}{\pi^2} \sum_{n=1}^{\infty} \frac{\exp(-n^2 B_t)}{n^2} \quad (4)$$

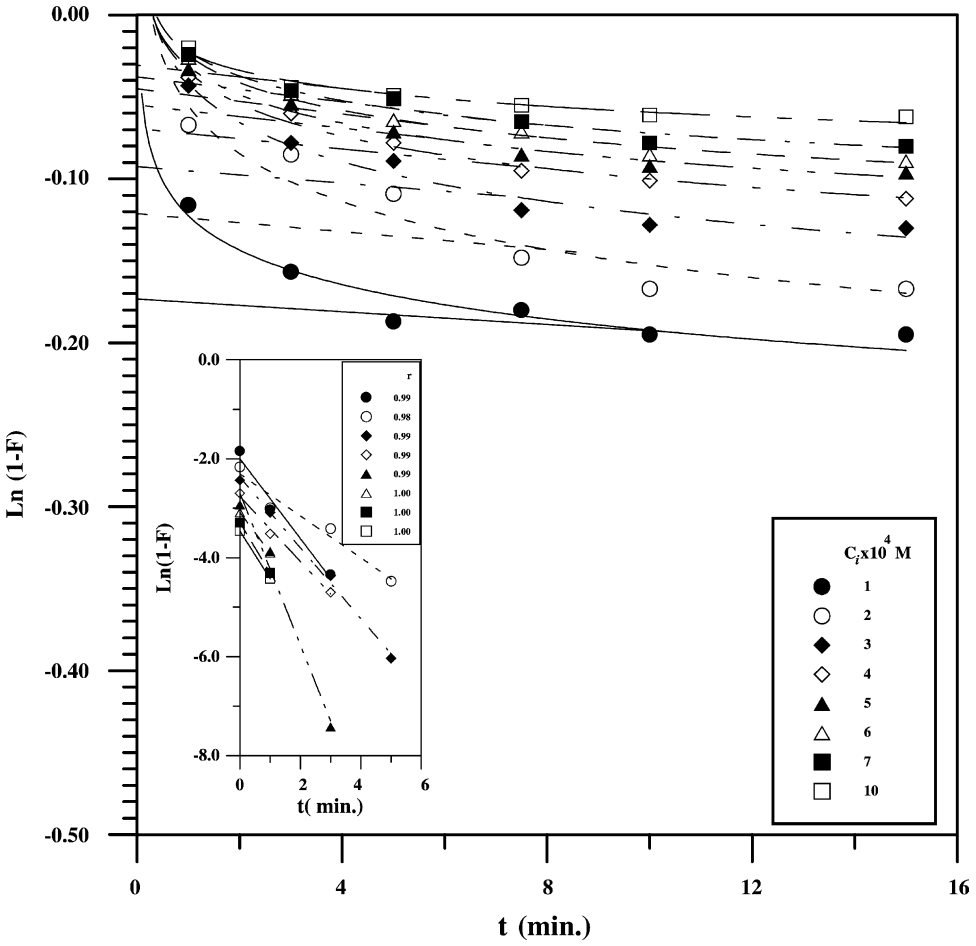

Fig. 4. McKay plots for CA adsorption on GP at various initial concentrations in the range of 1×10^{-4} to 1×10^{-3} M at 293 K (correlation coefficients for initial fast reaction are shown on the right corner in the small figure).

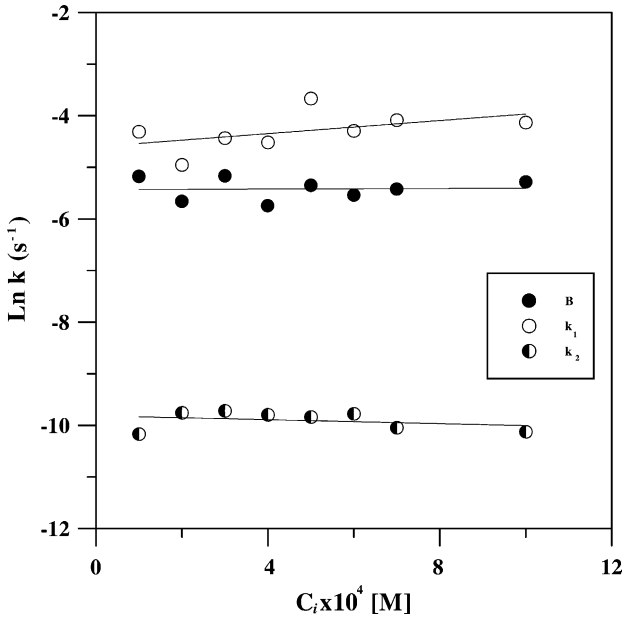

Fig. 5. The change of rate constants and B values with initial concentration of CA solutions at 293 K.

where Q_t and Q_∞ are the amounts of adsorbed dye at time t and at equilibrium, respectively. B, the time coordinate, is defined by

$$B = \frac{\pi^2}{r^2} D_\mathrm{i} \tag{5}$$

where D_i is the effective diffusion coefficient of the adsorbing ions. For every observed value of F', corresponding Bt values can be obtained from the Reichenberg table [26]. It has been found that the values of B determined from the Bt versus t plots shown in Fig. 6 are not affected by varying the initial dye concentration (see Fig. 5).

3.2. Effect of temperature on adsorption rate

A series of experiments have been conducted at 5×10^{-4} M dye concentration at 293, 303, 313 and 323 K to study effect of temperature on adsorption rate. Figs. 7 and 8 depict the effect of contact time on the rate of adsorption at four different temperatures. The rate constants and diffusion coefficients have been found to increase as the temperature is raised.

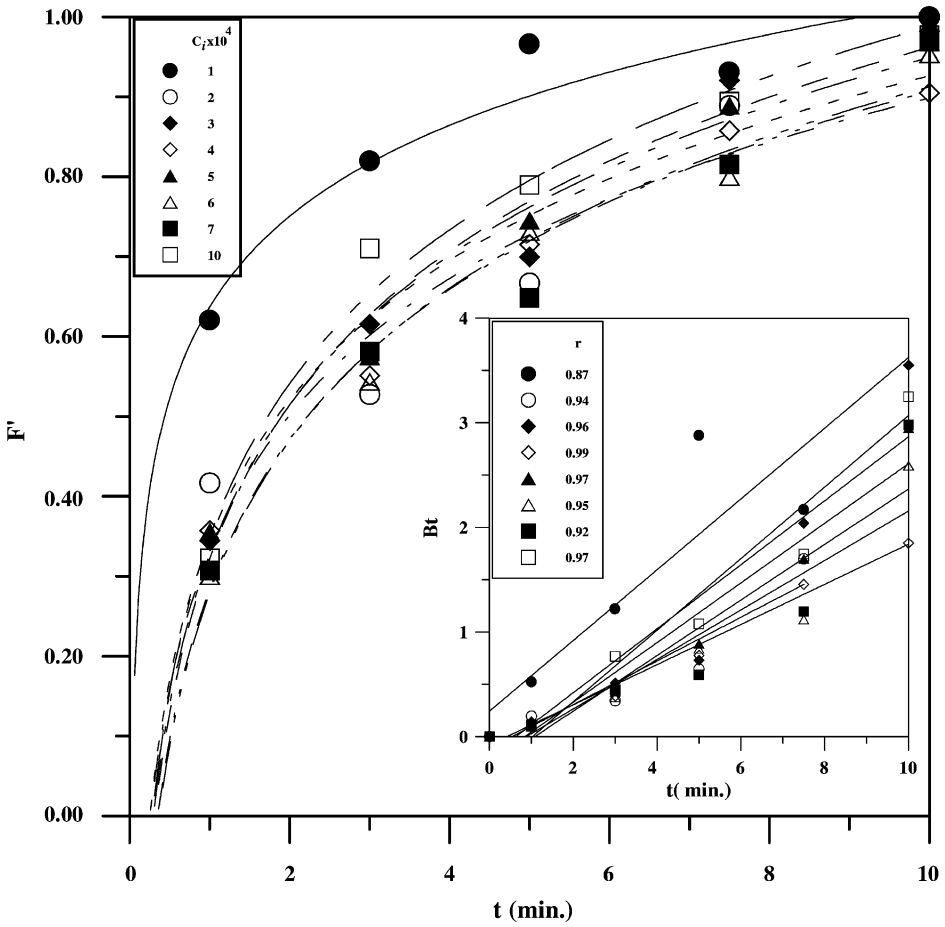

Fig. 6. Dependencies of the CA adsorption fractional attainment and *Bt* on time for various initial concentrations in the range of 1×10^{-4} to 1×10^{-3} M at 293 K.

Activation energies, E_a, for CA adsorption have been evaluated from the slopes of the $\ln k$ or $\ln D_i$ versus $1/T$ plots shown in Fig. 9 by using following Arrhenius equations:

$$\ln k = \ln A - \frac{E_a}{RT} \quad (6)$$

$$\ln D_i = \ln D_0 - \frac{E_a}{RT} \quad (7)$$

The entropy of activation ΔS^* and enthalpy of activation ΔH^* were also determined from the intercepts and the slopes of the linear plots shown in Fig. 9 according to the Eyring equation:

$$\ln \frac{k}{T} = \ln \frac{R}{Nh} + \frac{\Delta S^*}{R} - \frac{\Delta H^*}{RT} \quad (8)$$

where k is the rate constant, T the absolute temperature (K), R the gas constant (kJ mol^{-1} K^{-1}), h the Planck constant and N is Avogadro's number.

Gibbs free energy of activation, ΔG^*, was calculated from the well-known Eq. (9). All thermodynamic parameters are presented in Table 1.

$$\Delta G^* = \Delta H^* - T\,\Delta S^* \quad (9)$$

As is seen from Table 1, the positive values of E_a, ΔH^* and ΔG^* indicate the presence of an energy barrier in the adsorption process. The positive values for these parameters are quite common because the activated complex in the transition state is in an excited form. Similar results for activation parameters have also been reported for dye and protein adsorption onto silica, but the authors provided no explanation for their reasoning [27,28]. Here, various assumptions have been made to explain and interpret these results. Due to its near point of zero charge (3.97), the electrical double layer at the interface of GP disappears when in contact with solution at pH 4. This allows for both anion and cation adsorption. At pH values near pH_{pzc}, the GP surface can be charged both positively and negatively. The surface of SiO_2 at pH 4 is negatively charged while all of the other oxides of glass are positively charged [29,30]. Electroneutrality requires that overall surface charge is equal to zero at pH_{pzc} of GP. CA is an anionic dye that contains a carboxylic acid and phenolic groups. In aqueous solution, it ionizes to an anionic, colored component and H^+ cations. The anionic group is attracted to the positively charged SOH_2^+ sites. The acidic dye anion will suffer Coulombic repulsion upon approaching the surface due to the presence of SO^-

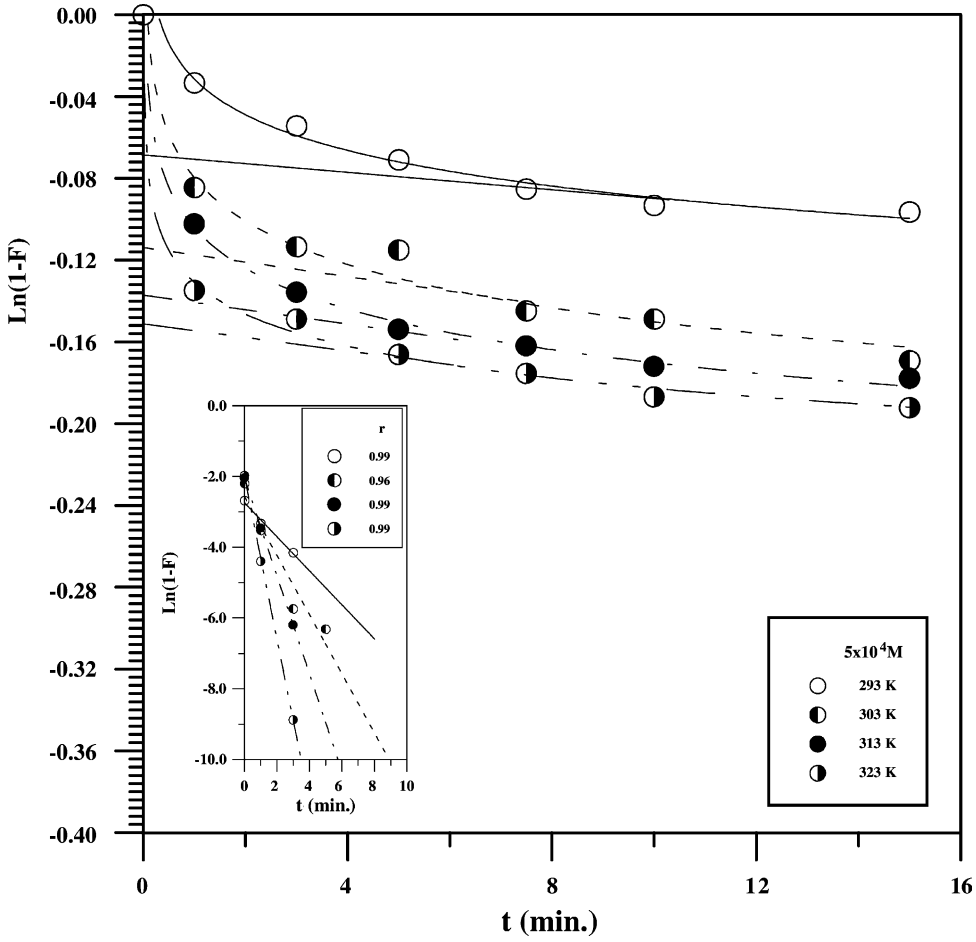

Fig. 7. Temperature dependencies of McKay plots at 5×10^{-4} M concentration of CA.

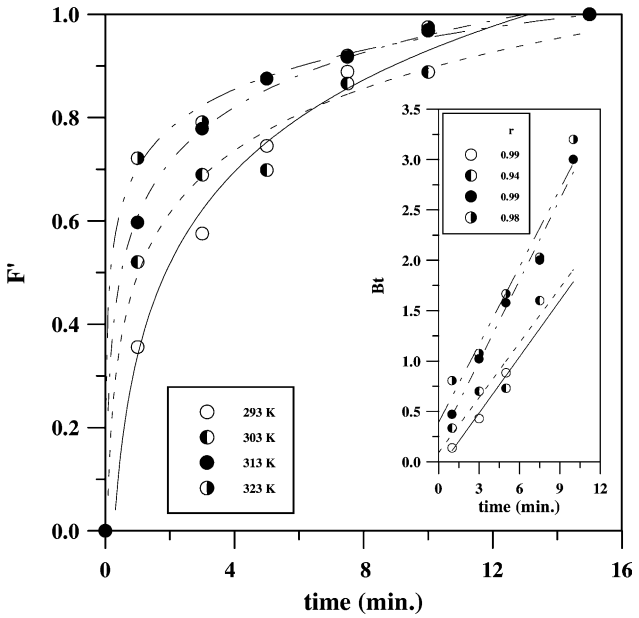

Fig. 8. Temperature dependencies of fractional attainment and *Bt* vs. *t* plots at 5×10^{-4} M concentration of CA.

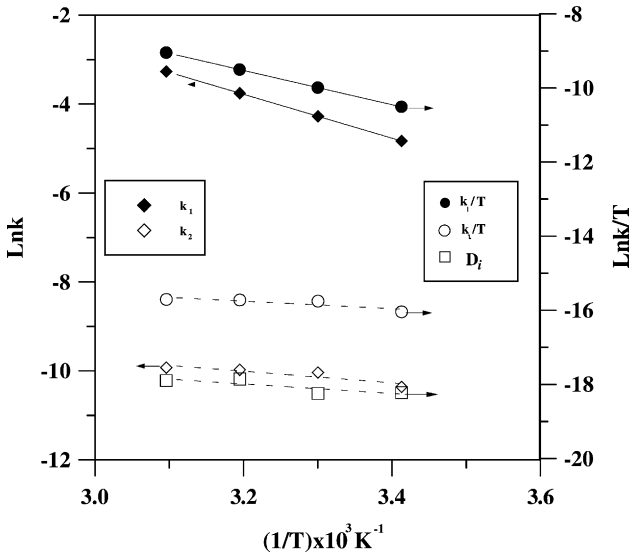

Fig. 9. Arrhenius and Eyring's plots for CA adsorption on GP (arrows indicate the appropriate axis).

Table 1
Activation energy parameters for adsorption of CA on GP

E_a (kJ mol^{-1})	r	ΔH^* (kJ mol^{-1})	r	ΔS^* (kJ mol^{-1} K^{-1})	T (K)	ΔG^* (kJ mol^{-1})
First step						
41.01	0.99	38.45	1.00	−0.15	293	84.96
					303	45.45
					313	46.95
					323	48.45
Second step						
10.86	0.91	8.28	0.86	−0.30	293	96.18
					303	99.18
					313	102.18
					323	105.18

groups on glass surface [31]. The energy barrier in for the activated state may arise partially from this repulsion. It has been reported that anionic species can adsorb to the glass and increase the negative charge on the surface [17]. On the other hand, in acetate buffer medium, acetate anions will compete with dye anions for adsorption sites. Since acetate anions are much smaller than CA, they may preferentially adsorb on adsorption sites in mesopores. Furthermore, the acetate concentration of 0.1 M is much larger than the CA concentration, and the activated complex is in equilibrium with these reactants. An ion-exchange reaction between CA and acetate ions which is favors acetate ions may partially contribute to the positive value of ΔG^*. The negative values of ΔS^* indicate that, as a result of CA adsorption, no significant changes occur in the internal structure of the GP.

The value of D_0 estimated from the plot of $\ln D_i$ versus $1/T$ is 9.6×10^{-7} cm^2 s^{-1} which correlates to effective diffusivities of 1.0×10^{-7} and 8.0×10^{-7} cm^2 s^{-1} for the adsorption of Deorlene Yellow and Telon Blue, respectively [12].

3.3. Adsorption isotherms

The adsorption data obtained for equilibrium conditions have been analyzed by using the following linear forms of the Freundlich and Langmuir isotherms (results are depicted in Fig. 10).

Freundlich isotherm:

$$\log Q = \log k_F + n \log C \quad (10)$$

where k_F is the Freundlich constant (a rough measure of adsorption capacity) and n an indicator of adsorption effectiveness. The n values, $0 < n < 1$, dictate favorable adsorption. As shown from the isotherm parameters in Table 2, adsorption data are well defined by a Freundlich isotherm with Freundlich exponent n less than unity.

Langmuir isotherm:

$$\frac{C}{Q} = \frac{1}{KQ_m} + \frac{C}{Q_m} \quad (11)$$

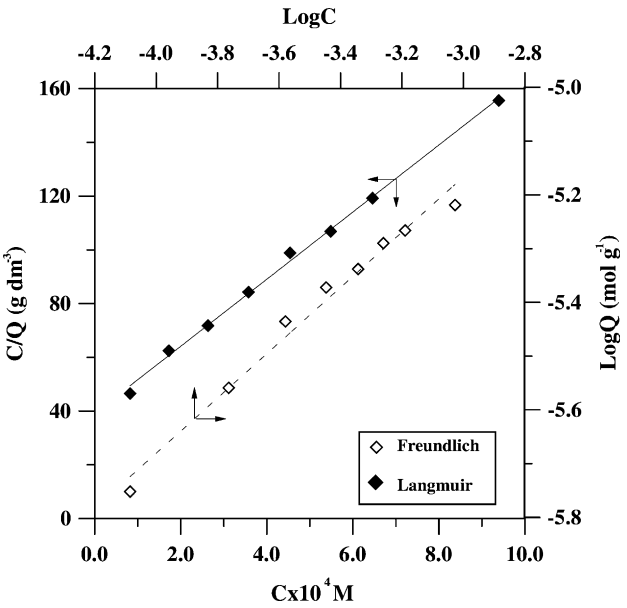

Fig. 10. Freundlich and Langmuir isotherm plots for CA adsorption with initial concentrations in the range of 1×10^{-4} to 1×10^{-3} M at 293 K (arrows indicate the appropriate axis).

where K and Q_m are the adsorption equilibrium constant and maximum adsorption capacity. The adsorption capacity of adsorbent and equilibrium constant has been derived from the Langmuir isotherm as 8.22×10^{-3} mmol g^{-1} (i.e. 4.03 mg g^{-1}) and 2.96×10^3 dm^3 mol^{-1}, respectively. The capacity of GP for CA is comparable to those found for

Table 2
Isotherm parameters for adsorption of CA on GP

Freundlich	
k_F (mmol g^{-1})	0.237
n	0.514
r	0.991
Langmuir	
K_L (dm^3 g^{-1})	2.40×10^{-2}
K (dm^3 mol^{-1})	2.96×10^3
Q_m (mmol g^{-1})	8.22×10^{-3}
r	0.998

the adsorption of Congo Red on red mud which involves various hydrous oxides [19], for Acid Red 91 on peat [21] and for some phenolic compounds on glass powder [32]. If the equilibrium concentration (C) is referenced to a standard concentration $C^0 = 1\,\mathrm{mol\,dm^{-3}}$, the adsorption equilibrium constant (K) is found to be dimensionless. The standard free energy of adsorption is calculated from the relationship $\Delta G^\circ = -RT\ln K$ to be $-19.5\,\mathrm{kJ\,mol^{-1}}$. The negative value of ΔG° indicates that adsorption process is spontaneous. The Langmuir constant, K_L, is defined as $K_\mathrm{L} = K \times Q_\mathrm{m}$. Further, the essential characteristics of the Langmuir isotherm are defined by a dimensionless separation factor, R_L, which is defined by the following relationship [33]:

$$R_\mathrm{L} = \frac{1}{1 + KC_\mathrm{i}} \tag{12}$$

The values of R_L have been found to be between 0 and 1, indicating favorable adsorption for CA on GP for the entire concentration range studied.

4. Conclusions

The experimental results described here show that GP has a potential for the removal of acid dyes from colored effluents. Although it is beyond the scope of this study, GP also holds promise for use in pigment preparation. Kinetic results showed that both film- and particle-diffusion are effective adsorption mechanisms. Both of the Freundlich and Langmuir isotherms gave good agreement with the experimental equilibrium data for the adsorption of dye onto glass. The kinetic and equilibrium data may be useful in designing treatment plants for removal of acid dyes from aqueous effluents.

Acknowledgements

This work supported by Research Fund of the University of Istanbul, Projects B-647/17072000.

References

[1] G. Wu, A. Koliadima, Y.S. Her, E. Mathievic, Adsorption of dyes on nanosize modified silica particles, J. Coll. Interf. Sci. 195 (1997) 222–228.
[2] G. Lagaly, K. Beneke, Interaction of exchange reactions of clay minerals and non-clay layer compounds, Coll. Polym. Sci. 269 (1991) 1198–1211.
[3] J.G. Hudleston, H.D. Willauer, K.R. Boaz, R.D. Rogers, Separation and recovery of food coloring dyes using aqueous biphasic extraction chromatographic resins, J. Chromatogr. B 711 (1998) 237–244.
[4] U. Sahm, D. Knittel, E. Schollmeyer, Electrochemical investigations on the analysis of reactive dyes with monoazoquinone and monoanthraquinone structures, Fresenius' J. Anal. Chem. 338 (7) (1990) 824–830.
[5] M. Valnice, B. Zanoni, A.G. Fogg, J. Barek, J. Zima, Electrochemical investigations of reactive dyes polarographic determination of anthraquinone-based chlorotriazine dyes, Anal. Chim. Acta 315 (1995) 41–54.
[6] J. Revenga, F. Rodriguez, J. Tijero, Study of redox behavior of anthraquinone in aqueous medium, J. Electrochem. Soc. 141 (2) (1994) 330–333.
[7] G.A. Qureshi, G. Svehla, M.A. Leonard, Electrochemical studies of strongly chelating anthraquinone derivatives, The Analyst 104 (1979) 705–721.
[8] G. Atun, M. Tuncay, G. Hisarli, Polarographic studies of non-ions surfactants with reference their structural influence on surface activity, Coll. Surf. A 113 (1996) 61–66.
[9] A. Wahl, N.A. Bonner, Radioactivity Applied to Chemistry, Wiley, New York, 1958.
[10] G.E. Boyd, A.W. Adamson, L.S. Myers, The exchange adsorptions of ions from aqueous solutions by organic zeolites. II. Kinetics, J. Am. Chem. Soc. 69 (11) (1947) 2836–2848.
[11] G. Atun, T. Sismanoglu, Adsorption of 4,4′-isopropylidene diphenol and dipenylol propane 4,4′-dioxyaceticacid from aqueous solution on kaolinite, J. Environ. Sci. Health A 31 (8) (1996) 2055–2069.
[12] G. McKay, M.S. Otterbrun, J.A. Aga, Pore diffusion and external mass transport during dye adsorption on to fuller's earth and silica, J. Chem. Tech. Biotechnol. 37 (1987) 247–256.
[13] G. MacKay, M.S. Otterbrun, J.A. Aga, Two resistance mass transport for the adsorption of dyes of fuller's earth, Water, Air and Soil Pollut. 33 (1987) 419–433.
[14] G. MacKay, Application of surface diffusion model to the adsorption of dyes on baggase pith, Adsorption 4 (1998) 361–372.
[15] G. MacKay, Adsorption of acid dye onto woodmeal by solid diffusional mass transfer, Chem. Eng. Process 19 (1985) 287–295.
[16] Z. Al-Qodach, Adsorption of dyes using shale oil ash, Wat. Res. 34 (17) (2000) 4295–4303.
[17] M.D. Rebolras, M. Kaszuba, M.T. Connah, M.N. Jones, Measurements of wall zeta potentials and their time-dependent changes due to adsorption processes: liposome adsorption on glass, Langmuir 17 (2001) 5314–5318.
[18] G. Atun, G. Hisarli, M. Tuncay, Adsorption of safranine-O on hydrophilic and hydrophobic glass surfaces, Coll. Surf. A 143 (1998) 27–33.
[19] C. Namasivayam, D.J.S.E. Arasi, Removal of congo red from wastewater onto waste red mud, Chemosphere 34 (2) (1997) 401–417.
[20] G.M. Walker, L.R. Weatherley, Adsorption of dyes from aqueous solution—the effect of adsorbent pore size distribution and dye aggregation, Chem. Eng. J. 83 (2001) 201–206.
[21] K.R. Ramakrishna, T. Viraraghavan, Dye removal using low cost adsorbents, Wat. Sci. Tech. 36 (2–3) (1997) 189–196.
[22] J. Wang, C.P. Huang, H.E. Allen, D.K. Cha, D.W. Kim, Adsorption characteristics of dye onto sludge particles, J. Coll. Interf. Sci. 208 (1998) 518–528.
[23] F. Delval, G. Crini, N. Morin, J. Vebrel, S. Bertini, G. Torri, The sorption of several tye dyes ofn crosslinked polysaccharides derivatives, Dyes and Pigments 53 (2002) 79–92.
[24] G.M. Walker, L.R. Weatherley, Fixed bed adsorption of acid dyes onto activated carbon, Environ. Pollut. 99 (1998) 133–136.
[25] N. Kannan, M.M. Sundaram, Kinetics and mechanism of removal of methylene blue by adsorption of various carbons—a comperative study, Dyes and Pigments 51 (2001) 25–40.
[26] D. Reichenberg, Properties of ion-exchange resins in relation to their structure. III. Kinetics of exchange, J. Am. Chem. Soc. 75 (1953) 589–597.
[27] S.K. Parida, B.K. Mishra, Adsorption of styril pyridinium dyes on silica gel, J. Coll. Interf. Sci. 182 (1996) 473–477.
[28] D. Sarkar, C.K. Chattoraj, Activation parameters for kinetics of protein adsorption, J. Coll. Interf. Sci. 157 (1993) 219–226.

[29] M.A. Anderson, J.A. Rubin, Adsorption of Inorganics at Solid Liquid Interfaces, Ann Arbor Science, Ann Arbor, MI, 1981.
[30] G. Atun, G. Hisarli, Surface properties of red mud by potentiometric method, J. Coll. Interf. Sci. 228 (2000) 40–45.
[31] G. McKay, M. El-Geundy, M.M. Nassar, Equilibrium studies on baggase pith, Adsorption Sci. Tecnol. 15 (4) (1997) 251–269.
[32] G. Atun, The adsorption of nitrophenols on a special adsorbent prepared from glass powder, Spectrosc. Lett. 25 (5) (1992) 741–756.
[33] T.W. Weber, R.K. Chakkravorty, Pore and solid diffusion models for fixed-bed adsorbers, AIChE J. 20 (1974) 228.